539.422.25

Criteria of Ductile Fracture Strain*

By Moriya OYANE**

Two criteria of ductile fracture strain are suggested. From the theory of plasticity for porous materials, the following criterion of fracture for a triaxial state of stress is obtained:

$$\int_0^{\varepsilon_{eqf}} \left(1+\frac{1}{a_0}\frac{\sigma_m}{\sigma_{eq}}\right) d\varepsilon_{eq} = b_0$$

where ε_{eqf} is the equivalent fracture strain, σ_m the mean stress, σ_{eq} the equivalent stress, a_0 and b_0 are constants. Except under certain conditions, this criterion shows reasonable agreement with experiment. To improve the accuracy of the prediction of the fracture strain, the above criterion is modified as follows:

$$\int_0^{\varepsilon_{eqf}} \left(1+\frac{1}{a_0}\frac{\sigma_m}{\sigma_{eq}}\right) \varepsilon_{eq}^{c_0} d\varepsilon_{eq} = b_0$$

where c_0 is a constant. It is found that this criterion provides a greater accuracy for prediction of the fracture strain.

1. Introduction

Since the main purpose of metal forming is to deform ductile metals without fracturing them, it is necessary to know the fracture strain of metals in the respective forming processes beforehand. It is clear that the differences in the stress systems applied by different processes, as well as the variation in working conditions, cause differences in fracture strain. The fracture strain may be affected by the histories of stress, strain, strain rate and temperature during plastic deformation. In this report, two criteria are suggested for predicting fracture strain from known relationships between equivalent strain and the principal stresses σ_1, σ_2 and σ_3. For simplicity, it is assumed that temperature and strain rate do not vary during deformation, and that the axes of principal stresses are fixed in the material.

2. Stages of ductile fracture

It is generally accepted that ductile fracture occurs in the following stages:

(1) After a certain plastic strain, microscopic holes, i.e., voids or cracks, may be nucleated at the edges of inclusions, precipitates and second phases, also they may be nucleated at grain boundaries or cell walls, by the interaction of the macroscopic stress and the microscopic stress concentrations due to piled-up dislocations [see Fig. 1(a) and (b)].

(2) The voids grow as the plastic strain increases, and the distance in the material between one void and another becomes smaller [see Fig. 1(c)].

(3) When the volume fraction of voids or the distance between the voids reaches a certain value, the plastic deformation is concentrated only into narrow regions which interconnect many holes [Fig. 1(d)], and macroscopic uniform deformation ceases.

(4) Separation occurs along these regions, and many dimple patterns can be observed on the fracture surface resulting from voids [Fig. 1(e)].

For stages (3) and (4), many models have been

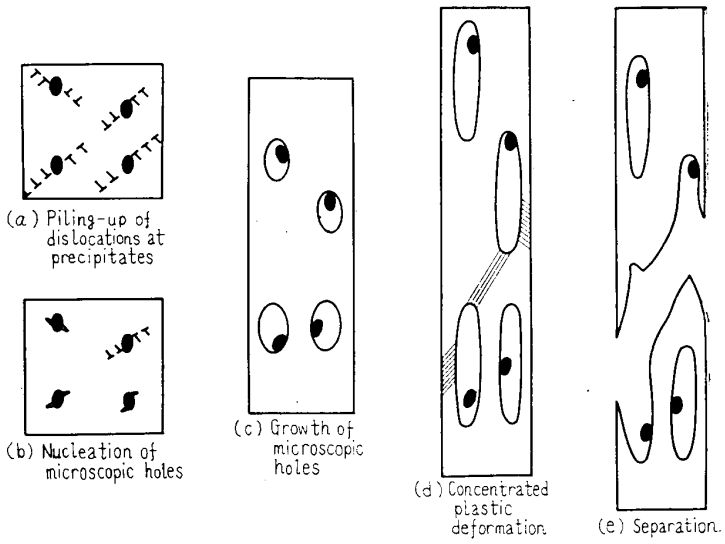

Fig. 1 Stages of ductile fracture

* Received 26th October, 1971.
** Professor, Faculty of Engineering, Kyoto University, Sakyo-ku, Kyoto.

proposed, i.e., internal necking, propagation of cracks and shear fracture.

One or two of these stages may not take place depending on the properties of the metal and the stress state. For example, a porous material need have no stage (1) and an equi-tensile stress $\sigma_1 = \sigma_2 = \sigma_3 > 0$ may allow fracturing in the absence of stage (2).

Some experimental evidence related with these stages is described below.

H. Sekiguchi et al.[1] observed voids around the fracture surface of a copper tensile specimen as shown in Fig. 2. Sekiguchi also showed in another report that for spheroidised carbon steel the voids are nucleated at the carbide precipitates as shown in Fig. 3. Figure 4 shows a density drop obtained in drawing by L. F. Coffin et al.[2] The reduction in area per pass in the drawing operation is 27% and the density of 6061-T6 aluminium alloy drops as the number of passes increases because the microscopic voids grow with an increasing plastic strain. Figure 5 shows two electronmicrographs of dimple patterns on the fracture surface of a copper tensile specimen taken by K. Showaki[3].

3. Survey of criteria of ductile fracture

Although it is desirable in a criterion of ductile fracture to take into account all the four stages listed above, such a complete solution is extremely difficult. For the prediction of the fracture strain in metal forming processes, only macroscopically uniform strain is important. It is unnecessary to consider the strain in later stages (3) and (4). In the experimental results the strain in stages (3) and (4) is included in the measured macroscopic strain, but the effect of this strain on the total strain is small

Fig. 2 Voids in a copper tensile specimen. Centre of fracture surface (Magnification = ×140)

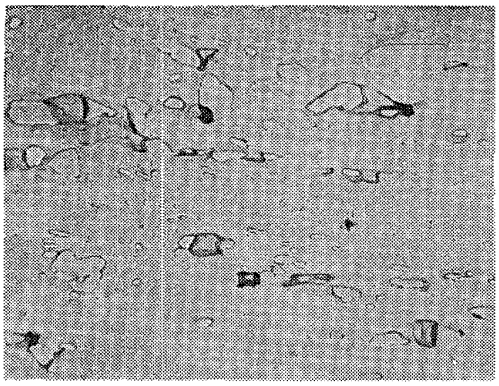

Fig. 3 Voids in spheroidised carbon steel (0.45% C, Tensile strain = 0.85, Magnification = ×2 000)

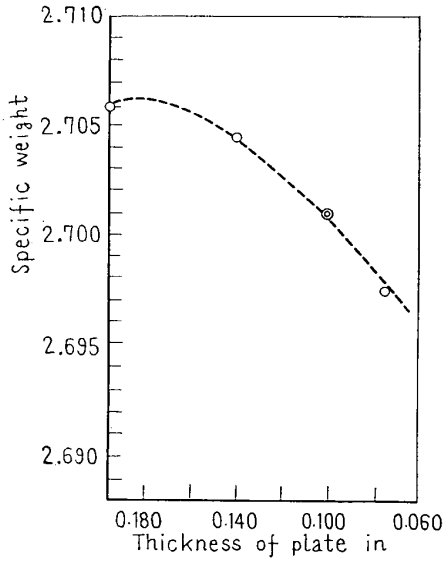

Material: 6061-T6 alminium

Fig. 4 Relationship between thickness of strip and density specific weight after successive drawing

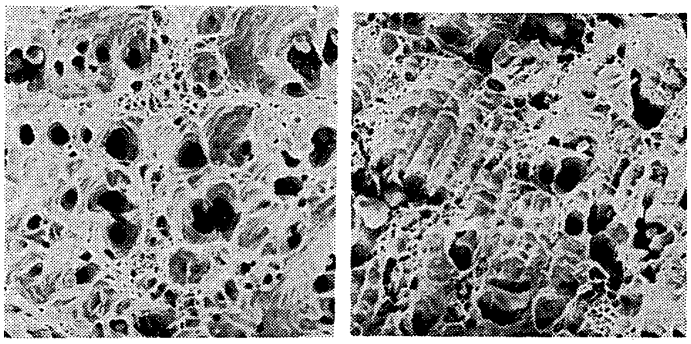

(a) from the position I (b) from the position II

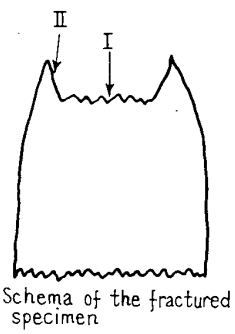

Fig. 5 Electronmicrographs of dimple patterns on the fracture surface of a copper tensile specimen (Magnification = ×3 750)

because of the concentration of the strain in very narrow regions.

To calculate the strain for stages (1) and (2), theories for the nucleation and growth of voids are necessary. To the author's knowledge, however, no theory which determines the amount of plastic strain before the nucleation of microscopic voids has been developed, whilst several criteria have been proposed assuming the existence of voids at the beginning of plastic deformation.

J. Gurland et al.[4] found a relationship between fracture strain and the volume fraction of inclusions, precipitates and microscopic voids for the simple tensile test. P. F. Thomason[5] proposed a theory of internal necking assuming the material between the voids to be two-dimensional, and suggested a criterion involving plastic strain before internal necking as a function of hydrostatic pressure.

For three-dimensional stress states, M. G. Cockcroft et al.[6] and K. Osakada et al.[9] proposed criteria considering the history of the maximum stress and the history of the hydrostatic stress component during deformation, respectively. F. A. McClintock et al.[7] derived a theory of ductile fracture strain for three-dimensional stress states using an analogy with the growth of a cylindrical hole in a two-dimensional material. However, the validity of the analogy of dynamics is not clear because the basic equations of hydrodynamics concern only a two-dimensional stream whilst the plastic model is three-dimensional.

The author has proposed a theory for plastic deformation of a metal with many spherical voids, and the present criteria of ductile fracture are developed based on this theory.

4. Outline of the theory of plasticity for a porous material[8]

Consider a porous material being deformed by principal stresses σ_1, σ_2 and σ_3. The incremental strains associated with the principal stress directions are $d\varepsilon_1$, $d\varepsilon_2$, and $d\varepsilon_3$. And the volumetric strain increment is $d\varepsilon_v$. The stress-strain relations are expressed by

$$\left.\begin{aligned} d\varepsilon_1-\frac{d\varepsilon_v}{3}&=\frac{d\varepsilon_{eq}}{\gamma\sigma_{eq}}\left(\sigma_1-\frac{\sigma_2}{2}-\frac{\sigma_3}{2}\right)\\ d\varepsilon_2-\frac{d\varepsilon_v}{3}&=\frac{d\varepsilon_{eq}}{\gamma\sigma_{eq}}\left(\sigma_2-\frac{\sigma_3}{2}-\frac{\sigma_1}{2}\right)\\ d\varepsilon_3-\frac{d\varepsilon_v}{3}&=\frac{d\varepsilon_{eq}}{\gamma\sigma_{eq}}\left(\sigma_3-\frac{\sigma_1}{2}-\frac{\sigma_2}{2}\right)\\ d\varepsilon_v&=\frac{d\varepsilon_{eq}}{\gamma f^2}\left(\frac{\sigma_m}{\sigma_{eq}}+a_0\right)\end{aligned}\right\} \quad \cdots\cdots(1)$$

where γ is the relative density obtained by dividing the nominal density ρ of the porous material, by the density ρ_0 of the constituent metal of the porous material. f is a function of γ only and it has been shown by experiment that f may be expressed as

$$f=\frac{1}{3}\left(1+\sqrt{\frac{\gamma}{1-\gamma}}\right) \quad \cdots\cdots(2)$$

σ_{eq} and $d\varepsilon_{eq}$ are the equivalent flow stress and equivalent strain increment of the constituent material, respectively. σ_m is the hydrostatic stress and a_0 is a material constant. σ_m, $d\varepsilon_v$, $d\varepsilon_{eq}$ and σ_{eq} are defined as follows*:

$$\sigma_m=\frac{1}{3}(\sigma_1+\sigma_2+\sigma_3) \quad \cdots\cdots(3)$$

$$d\varepsilon_v=d\varepsilon_1+d\varepsilon_2+d\varepsilon_3 \quad \cdots\cdots(4)$$

$$(d\varepsilon_{eq})^2=\frac{2}{9}\{(d\varepsilon_1-d\varepsilon_2)^2+(d\varepsilon_2-d\varepsilon_3)^2+(d\varepsilon_3-d\varepsilon_1)^2\} \quad \cdots\cdots(5)$$

$$(\sigma_{eq})^2=\frac{1}{2}\{(\sigma_1-\sigma_2)^2+(\sigma_2-\sigma_3)^2+(\sigma_3-\sigma_1)^2\} \quad \cdots\cdots(6)$$

For a material with no voids, the value of γ is unity and the value of f is infinity, so that these equations are consistent with the Mises yield criterion and the Lévy-Mises equation.

The volumetric strain, whose incremental form is expressed by Eq. (4), is defined by

$$\varepsilon_v=\ln\frac{v}{v_0}=-\ln\frac{\rho}{\rho_0}=-\ln\gamma \quad \cdots\cdots(7)$$

where v is the volume of the porous material and v_0 is the volume of the constituent metal of the same weight. Therefore, according to this definition of the volumetric strain, a porous material has a volumetric strain even before being deformed.

5. Criteria of fracture strain

As mentioned in section 2, ductile fracture progresses gradually as the plastic strain increases. If the end of stage (2) or the end of uniform straining is defined as the fracture point, the beginning of stage (3) is the condition of fracture. As a first approximation, let us assume that stage (3) begins when the relative density, γ, decreases to a certain value or when the volumetric strain reaches a certain value.

Figure 6[9] shows a relationship between the density of grey cast iron and the compressive strain for high pressures. The density decreases as the compressive strain increases and macroscopic fracture has occurred at the crosses in the figure. This figure suggests that fracture occurs when the relative density decreases to approximately 0.94, and this result appears to support the above assumption. From the fourth equation of Eq. (1),

* As shown in the original paper[8], $d\varepsilon_{eq}$ and σ_{eq} include the terms $d\varepsilon_v$ and σ_m/f respectively. These terms are neglected in these equations because their values are very close to zero when γ is nearly unity as is the case in ductile fracture.

$$\frac{\gamma f^2}{a_0} d\varepsilon_v = \left(1+\frac{1}{a_0}\frac{\sigma_m}{\sigma_{eq}}\right) d\varepsilon_{eq} \quad \cdots\cdots(8)$$

Provided that fracture occurs at a volumetric strain of ε_{vf}, the fracture strain ε_{eqf} is given by integration of Eq. (8):

(i) For a porous material with an initial volumetric strain of ε_{v0}

$$\int_{\varepsilon_{v0}}^{\varepsilon_{vf}} \frac{\gamma f^2}{a_0} d\varepsilon_v = \int_0^{\varepsilon_{eqf}} \left(1+\frac{1}{a_0}\frac{\sigma_m}{\sigma_{eq}}\right) d\varepsilon_{eq} \quad \cdots\cdots(9\cdot1)$$

(ii) For a solid material ($\gamma=1$ and $\varepsilon_{v0}=0$) in which microscopic voids are nucleated as soon as plastic deformation begins,

$$\int_0^{\varepsilon_{vf}} \frac{\gamma f^2}{a_0} d\varepsilon_v = \int_0^{\varepsilon_{eqf}} \left(1+\frac{1}{a_0}\frac{\sigma_m}{\sigma_{eq}}\right) d\varepsilon_{eq} \quad \cdots\cdots(9\cdot2)$$

(iii) For a solid material ($\gamma=1$ and $\varepsilon_{v0}=0$) in which microscopic voids are nucleated after a certain equivalent plastic strain of ε_{eqi}

$$\int_0^{\varepsilon_{vf}} \frac{\gamma f^2}{a_0} d\varepsilon_v = \int_{\varepsilon_{eqi}}^{\varepsilon_{eqf}} \left(1+\frac{1}{a_0}\frac{\sigma_m}{\sigma_{eq}}\right) d\varepsilon_{eq} \quad \cdots\cdots(9\cdot3)$$

Because γ and f are functions of ε_v only as defined by Eq. (2) and Eq. (7), the terms on the left hand-sides of Eqs. (9·1) to (9·3) are functions of ε_{v0} and ε_{vf} only, i.e., the terms are material constants.

Since the equation which determines the strain of void nucleation, ε_{eqi}, is not clear as mentioned in section 2, only Eqs. (9·1) and (9·2) will be given further theoretical development. The possibility of a solution of (9·3) will be discussed in section 7. For comparison with the experimental results in section 6, the theoretical results with $\varepsilon_{eqi}=0$ will be used irrespective of material properties such as the volume, distribution and shape of porosity, inclusions and the like. Both Eqs. (9·1) and (9·2) lead to a simple expression for the fracture strain thus:

$$\int_0^{\varepsilon_{eqf}} \left(1+\frac{1}{a_0}\frac{\sigma_m}{\sigma_{eq}}\right) d\varepsilon_{eq} = b_0 \text{ (constant)} \quad \cdots\cdots(10)$$

or

$$\int_0^{\varepsilon_{eqf}} \left(a_0+\frac{\sigma_m}{\sigma_{eq}}\right) d\varepsilon_{eq} = a_0 b_0 \text{ (constant)} \quad \cdots\cdots(10)'$$

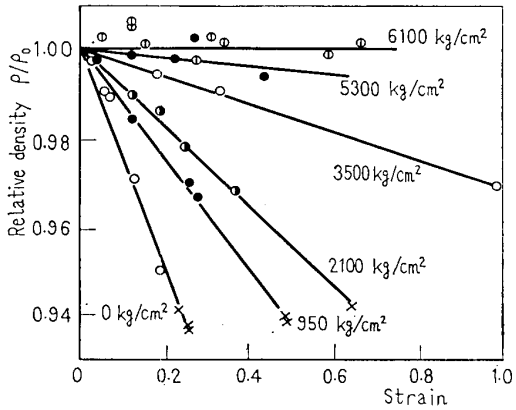

Fig. 6 Relationship between relative density of grey cast iron and compressive strain under high pressures

where a_0 and b_0 can be determined from experiments carried out under two different stress states.

As will be exhibited in the following section, this equation does not always provide enough accuracy for predicting the fracture strain. The discrepancies between theoretical and experimental results are considered to be due to the simplified assumption that fracture occurs when the volumetric strain reaches a certain value. As the plastic strain increases the stress-strain curve of the metal tends to have a lower slope and the dislocation density increases, so that stage (3), due to internal necking or crack propagation, may begin at a smaller volumetric strain. To take this effect into account, Eq. (10) is modified in the following way.

$$\int_0^{\varepsilon_{eqf}} \left(1+\frac{1}{a_0}\frac{\sigma_m}{\sigma_{eq}}\right) \varepsilon_{eq}{}^{c_0} d\varepsilon_{eq} = b_0 \quad \cdots\cdots(11)$$

The weighting factor ε_{eq} is used in the equation thereby increasing the accuracy of the determination of the fracture strain. For $c_0=0$, the weighting factor is constant throughout deformation and the equation is the same as Eq. (10). As the value of c_0 increases from zero, the stress states at larger strains have a greater effect on fracture than at smaller strains.

For a non work-hardening material, the following equation is obtained by substituting $\sigma_{eq}=\sigma_0$ into Eq. (11).

$$\int_0^{\varepsilon_{eqf}} \left(1+\frac{1}{a_0}\frac{\sigma_m}{\sigma_0}\right) \varepsilon_{eq}{}^{c_0} d\varepsilon_{eq} = b_0 \quad \cdots\cdots(12)$$

6. Comparison of the criteria with experimental results

6·1 Equation (10)

K. Osakada and H. Hayashi[9] investigated the effect of two-dimensional stress histories on the fracture strain of malleable cast iron. At first they conducted simple tension and compression tests and measured the fracture strain to determine the constants a_0 and b_0 in Eq. (10). The values of the hydrostatic stresses σ_m/σ_{eq} in these tests are 1/3 and $-1/3$ for tension and compression tests, respectively. The equation obtained is

$$\int_0^{\varepsilon_{eqf}} \left(1+2.5\frac{\sigma_m}{\sigma_{eq}}\right) d\varepsilon_{eq} = 0.23 \quad \cdots\cdots(13)$$

or

$$\int_0^{\varepsilon_{eqf}} \left(0.4+\frac{\sigma_m}{\sigma_{eq}}\right) d\varepsilon_{eq} = 0.09 \quad \cdots\cdots(13)'$$

To determine the effectiveness of this equation for predicting the fracture strain for general two-dimensional stress conditions, compression tests were performed using recessed dies causing a controlled barrelling. The specimens were subjected to simple tension and compression tests up to a strain of ε_p, and then compressed by the recessed dies. The stresses at the centre of the barrelled surface were measured

as shown in Fig. 7. Substituing this stress history into Eq. (13), the fracture strains were calculated.

Figure 8 illustrates the comparison between the calculated and the measured strain for the four different combinations of prestrains ε_p and histories of σ_1/σ_2. The calculated results agree quite well with the measured results, and this suggests that Eq. (10) agrees closely and is valid for this material. Equation (10) was used for copper and mild steel and a reasonable agreement is obtained for each material with experimental results.

6·2 Equation (12)

Although the simple expression of Eq. (10) can be applied to many metals, the agreement is not good under some conditions. For these cases, more sophisticated expressions derived from Eq. (11) provide more accurate agreement with experiment.

To illustrate this difference, Eq. (10) and Eq. (12) are compared for tensile tests under high pressure, in which the pressure changes from p_1 to p_2 at a certain strain of ε_1.

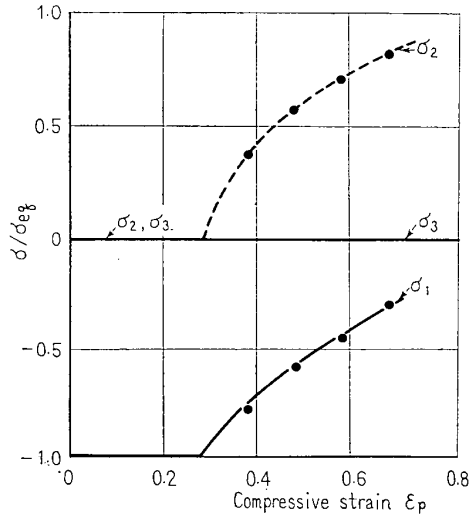

Fig. 7 An example of stress history midway between the dies along the outer surface during a compression test by smooth and successively by recessed dies

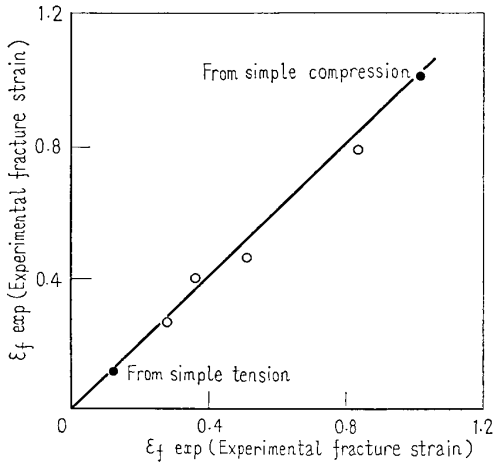

Fig. 8 Comparison of the calculated and experimental fracture strains

Supposing that the material has a constant flow stress σ_0 and that the flow stress is not affected by the hydrostatic stress component σ_m, the principal stresses during a tensile test under a pressure p are σ_0-p, $-p$ and $-p$, so that σ_m is

$$\sigma_m=\frac{1}{3}\sigma_0-p \quad \cdots\cdots(14)$$

The fracture strains ε_{f1} and ε_{f2} under constant pressures of p_1 and p_2 are expressed as follows from Eqs. (12) and (14).

$$\left.\begin{aligned}\int_0^{\varepsilon_{f1}}\left(1+\frac{1}{3a_0}-\frac{p_1}{a_0\sigma_0}\right)\varepsilon_{eq}{}^{c_0}d\varepsilon_{eq}=b_0\\ \int_0^{\varepsilon_{f2}}\left(1+\frac{1}{3a_0}-\frac{p_2}{a_0\sigma_0}\right)\varepsilon_{eq}{}^{c_0}d\varepsilon_{eq}=b_0\end{aligned}\right\} \quad \cdots\cdots(15)$$

For the case in which the circumferential pressure changes from p_1 to p_2 at a strain of ε_1 then:

$$\int_0^{\varepsilon_1}\left(1+\frac{1}{3a_0}-\frac{p_1}{a_0\sigma_0}\right)\varepsilon_{eq}{}^{c_0}d\varepsilon_{eq}+\int_{\varepsilon_1}^{\varepsilon_f}\left(1+\frac{1}{3a_0}-\frac{p_2}{a_0\sigma_0}\right)\varepsilon_{eq}{}^{c_0}d\varepsilon_{eq}=b_0 \quad \cdots\cdots(16)$$

Integrating Eqs. (15) and (16) and eliminating p_1 and p_2,

$$\left(\frac{1}{\varepsilon_{f1}{}^{c_0+1}}-\frac{1}{\varepsilon_{f2}{}^{c_0+1}}\right)\varepsilon_1{}^{c_0+1}+\left(\frac{\varepsilon_f}{\varepsilon_{f2}}\right)\varepsilon_2{}^{c_0+1}=1 \quad \cdots\cdots(17)$$

When $c_0=1$ in Eq. (17), if ε_1 is plotted against ε_f, then an elliptical relationship is produced when $\varepsilon_{f1}<\varepsilon_{f2}$ and a hyperbolic relationship is produced when $\varepsilon_{f1}>\varepsilon_{f2}$. When $c_0=0$ this equation is the same as Eq. (10), and the plot of ε_1 against ε_f is linear.

Equation (17) is compared with some experimental results assuming constant mean flow stresses instead of varying flow stresses.

Figures 9(a) and (b) show the results for copper obtained by H. Sekiguchi et al.[1] p_1 is zero (atmospheric pressure) and p_2 is 2700 kg/cm^2 for Fig. 9(a), whereas p_1 is 2700 kg/cm^2 and p_2 is zero for Fig. 9(b). The solid lines in the figures are calculated from Eq. (17) when $c_0=1$ using the measured values of ε_{f1} and ε_{f2}. These calculated results agree well with the experimental results.

Figure 10 shows a rearranged result of P. W. Bridgman's[10] experiments on tempered pearlitic steel and tempered martensitic steel. The tensile test specimens were stretched under high pressures and then stretched to fracture at atmospheric pressure. The solid lines in this figure are calculated from Eq. (17) with $c_0=1$. A satisfactory agreement between the experimental and calculated results is obtained.

The broken lines in Figs. 9(a), (b) and Fig. 10 are the straight lines calculated from Eq. (10) or

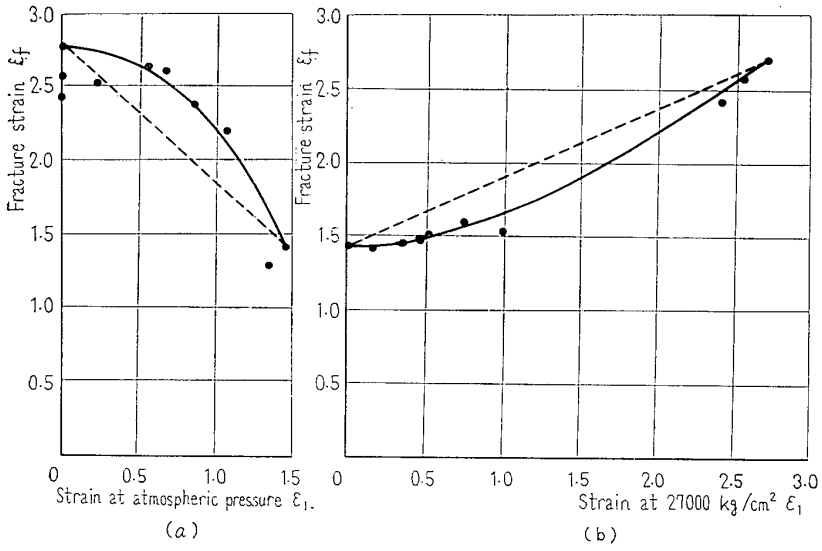

Fig. 9 Effect of superimposed pressure on the fracture strain of copper tensile specimens

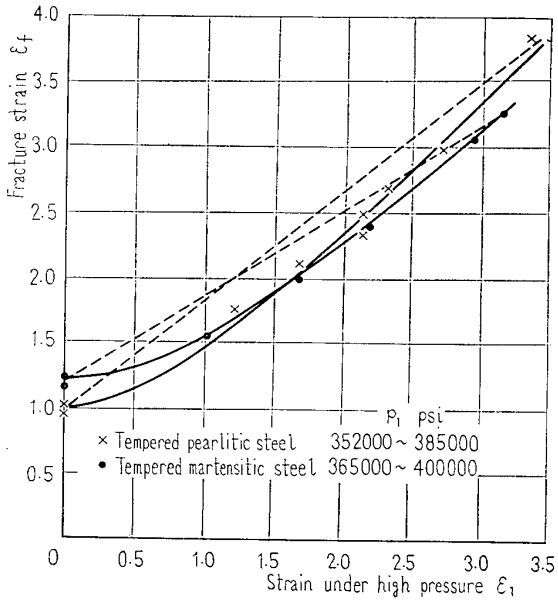

Fig. 10 Effect of superimposed pressure on the fractures strain of tempered pearlitic steel and tempered martensitic steel

from Eq. (17) with $c_0=0$. It is obvious that the accuracy of Eq. (10) is less than that of Eq. (11). However, Eq. (10) is easier to treat and is recommended for use when a very high accuracy is not required.

7. Discussion

In the process of developing the present fracture criteria, the strain ε_{eqi} of void nucleation is neglected. Equation (11) now has no physical meaning as c_0 was introduced to compensate the delay in the beginning of stage (3), though Eqs. from (9·1) to (9·3) were theoretically derived. Therefore the effectiveness of Eq. (11) will be determined by whether this equation provides good agreement with experimental results or not.

Although Eq. (11) gives an accurate prediction of fracture strain, it is clear that a complete equation which includes all the stages of nucleation, growth and coalescence of voids is desirable.

For predicting the strain ε_{eqi} of microscopic void nucleation, another criterion is necessary and it may be necessary to introduce the following relationships: a relationship between strain ε_{eqi} and the number of piled-up dislocations and a relationship among the required macroscopic stress, number of the piled-up dislocations and the intrinsic strength of inclusions, precipitates etc., and/or their bonding strength with the material.

On the other hand, for a delay in stage (3) to occur, it is necessary to consider the change in void shape and to develop the theory of internal necking or crack propagation with the assumed shape of voids and work-hardening characteristics and dislocation density.

8. Conclusions

(1) From the theory of plasticity for porous materials, the following criterion of ductile fracture strain is obtained;

$$\int_0^{\varepsilon_{eqf}} \left(1+\frac{1}{a_0}\frac{\sigma_m}{\sigma_{eq}}\right) d\varepsilon_{eq}=b_0$$

Except for some conditions discussed above, this criterion appears to agree well with the experimental results.

(2) To improve the accuracy of predicting the fracture strain, the above criterion is modified as follows;

$$\int_0^{\varepsilon_{eqf}} \left(1+\frac{1}{a_0}\frac{\sigma_m}{\sigma_{eq}}\right) \varepsilon_{eq}{}^{c_0} d\varepsilon_{eq}=b_0$$

From the comparisons with experiments, this criterion is found to provide an accurate prediction of fracture strain.

(3) It is suggested that studies involving the mechanics of the nucleation of microscopic voids and the conditions of internal necking and crack propagation are necessary for further development of the theory of ductile fracture.

Acknowledgement

The author is grateful for the kindness shown by Assistant Prof. K. Osakada and Mr. B. Dodd (Department of Industrial Metallurgy, University of Birmingham), who translated the present report into English.

References

(1) Sekiguchi, H., et al., *Preprint 21th Joint Congress on Metal Forming* (in Japanese), (1970), p. 115.
(2) Coffin, L.F. Jr., et al., *General Electric, Technical Information Series*, Metal Working No. 67-C-406, (1967-10).
(3) Showaki, K., *Jour. Japan Soc. Tech. Plasticity* (in Japanese), Vol. 13 No. 135 (1972-4), p. 235.
(4) Gurland, J., et al., *Trans. ASM*, Vol. 56 (1963), p. 442.
(5) Thomason, P.F., *Jour. Inst. Metals*, Vol. 96 (1968), p. 360.
(6) Cockcroft, M.G., et al., *Jour. Inst. Metal*, Vol. 96 (1968), p. 33.
(7) McClintock, F.A., *Trans. ASME*, Ser. E, Vol. 35, No. 2 (1968-6), p. 363.
(8) Oyane, M., et al., *Trans. Japan Soc. Mech. Engrs.* (in Japanese), Vol. 39, No. 318 (1973).
(9) Osakada, K., et al., *Jour. Japan Soc. Techn. Plasticity* (in Japanese), Vol. 12, No. 128 (1971-9), p.687.
(10) Bridgman, P.W., *Studies in Large Plastic Flow and Fracture*, (1964), p.300, Harvard University Press.